CHAPTER IV

Complex Ginzburg-Landau equation—(t

COMPLEX GINZBURG-LANDAU EQUATION

From this chapter on, we will study pattern formation in $1-d$ spatially extended systems from a periodic orbit theory point of view. The Kuramoto-Sivashinsky equation (KSe) and the complex Ginzburg-Landau equation (CGLe) are the prototyped equations in this investigation. In this chapter, we emphasiz the important role played by coherent structures in the dynamics of the CGLe which can be defined as the steady or traveling wave solutions. Basic properties of the CGLe are reviewed in sect. 4.1, and various coherent structures are defined and their importance is discussed in sect. 4.2. A new formulation of the steady solutions of the CGLe is presented in sect. 4.3 by which we proved the existence of the modulated-amplitude waves (MAWs) near the onset of instability. We compare the obtained analytical expression with the numerical calculation and discuss their stability as well in sect. 4.5.

4.1 Review

4.1.1 Introduction

The complex Ginzburg-Landau equation (CGLe) is a generic amplitude equation describing Hopf bifurcation in spatially extended systems, *i.e.*, I_o systems [46], with reflection symmetry [136, 225, 260]. It is of great interest due to its genericity and applications to onset of wave pattern-forming instabilities [46] in various physical systems such as fluid dynamics, optics, chemistry and biology. It exhibits rich dynamics and has become a paradigm for studying transitions to spatiotemporal chaos.

Consider the $1-d$ CGLe for the complex amplitude field $A(x,t)$:

$$A_t = \mu A + (1+i\alpha)A_{xx} - (1+i\beta)|A|^2 A\,, \tag{70}$$

where $A(x,t) : \mathbb{R}^2 \mapsto \mathbb{C}$, and $\mu, \alpha, \beta \in \mathbb{R}$, $x \in \mathcal{D}$. $\mathcal{D}$ is the spatial domain on which the equation is defined. A_t, A_{xx} denote repectively the first temporal derivative and the second spatial derivative of A. Interesting domains for us are either the whole real axis or a finite box of length L with periodic boundary conditions. μ is the control parameter. Only $\mu > 0$ is considered as we study the supercritical Ginzburg-Landau equation; one could set $\mu = 1$ by appropriate rescaling of the time, space and amplitude, but we keep it as a parameter for closer connection with experimental results and literature. Coefficients α and β parametrize the linear and nonlinear dispersion.

If both α and β are set to 0, we recover the real Ginzburg-Landau equation (GLe) in which only the diffusion term and the stabilizing cubic term compete with each other and

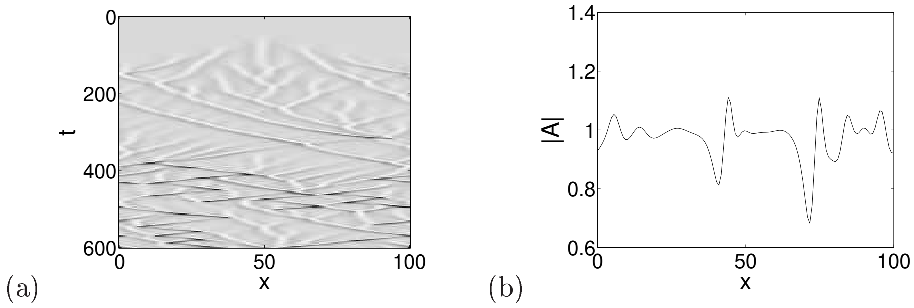

Figure 7: A typical evolution of the CGLe (70) in the chaotic regime in a periodic box with size $L = 100$. $\alpha = 1.5\,,\beta = -1.4\,,128$ Fourier modes used. (a) The space-time gray scale plot; (b) The spatial profile of $|A|$ at $t = 450$.

with the linear term. A Lyapunov functional exists in that case [46] and the GLe behaves like a gradient system. Another limit — the nonlinear Schrödinger equation — results from setting $\alpha, \beta \to \infty$; we then have an integrable nonlinear PDE with infinitely many conserved quantity. For parameter values in the intermediate range, the CGLe inherits partial properties of the gradient system and the conserved system, and long-time behavior of the CGLe can vary from stationary to periodic and to spatiotemporal chaos [229].

See figure 7 for a typical space-time evolution of the CGLe (70). In figure 7(a), structures are seen born out of the initial disturbances. They retain their identity and move steadily except at separate space-time points where they collide and annhilate, new structures being born. In figure 7(b), the spatial profile of $|A|$ at $t = 450$ is shown. Many oscillating structures are present and in fact they are closely related to the steady solutions of the CGLe in small periodic box, like plane waves, MAWs, solitary waves. The whole profile consists of patches of these simpler objects, the study of which is thus the first step towards understanding of pattern formation in the $1-d$ CGLe. We will concentrate on the stationary solutions of the CGLe in a finite box of length L with periodic boundary conditions, and the case $\alpha \neq \beta$. Stationary solutions are the simplest non-trivial solutions, related to propagating solutions by a change of frame of reference $(x,t) \mapsto (x - vt, t)$ with fixed $v \in \mathbb{R}$.

4.1.2 Symmetries and Bekki-Nozaki solutions

Equation (70) is invariant under temporal and spatial translations. Moreover, it is invariant under a global gauge transformation $A \to A\exp(i\phi)$, where $\phi \in \mathbb{R}$, and under $x \to -x$ reflection. As a consequence, it preserves the parity of A, i.e., if $A(-x,0) = \pm A(x,0)$, then $A(-x,t) = \pm A(x,t)$ for any later time $t > 0$. If $A(x,t)$ has no parity, then $A(-x,t)$ gives another solution.

For a spatially infinite system there exists a continuous family of traveling holes - the Bekki-Nozaki solution [15]. If we set $\xi = x - ct$, the position in the moving frame (c is the velocity to be determined later), then the Bekki-Nazakisolution is

$$A = \frac{b_1 e^{\kappa\xi} + b_2 e^{-\kappa\xi}}{e^{\kappa\xi} + e^{-\kappa\xi}} \exp\left(\frac{i}{2}\int_0^{\xi} (\kappa_+ + \kappa_- \tanh \kappa s)\, ds - i\Omega t\right), \tag{71}$$

where

$$\Omega = \alpha\mu - c\frac{\kappa_1\kappa_2}{\sqrt{\mu}}\,, \quad c = (\kappa_1+\kappa_2)(\alpha-\beta),$$
$$\kappa_\pm = \kappa_1 \pm \kappa_2\,, \quad \kappa = -\frac{\kappa_-}{2\alpha}; \quad |b_j|^2 = \mu - \kappa_j^2\,, \text{ for } j = 1,2,$$
$$\sigma \equiv \arg(\frac{b_2}{b_1}) = -\arctan\left(2\kappa_+\kappa_-\frac{p(\alpha-\beta)-\frac{1}{p}(1+\alpha\beta)}{(1+\beta^2)\kappa_+^2-(p^2+p^{-2})(1+\alpha^2)\kappa_-^2}\right),$$
$$p = -q \pm (2+q^2)^{\frac{1}{2}}\,, \quad q = -\frac{3}{2}\frac{1+\alpha\beta}{\alpha-\beta}.$$

The asymptotic wave-numbers (at $|\kappa\xi| \gg 1)\kappa_1$ and κ_2 satisfy

$$\frac{(\kappa_1+\kappa_2)^2}{a_1^2} + \frac{(\kappa_1-\kappa_2)^2}{a_2^2} = 1,$$

where

$$a_1^2 = 4\mu\left(1 - \frac{3p(1+\beta^2)}{(\alpha-\beta)(1+p^2)}\right)^{-1}\,, \quad a_2^2 = 4\mu\left(1 - \frac{3(1+\alpha^2)}{p(\alpha-\beta}\right)^{-1}.$$

A branch of p should be chosen so as to make a_1^2 and a_2^2 to be positive. The solution is highly unstable for α, β values we are considering here.

The one-parameter family of the hole solutions strongly suggest the existence of a hidden symmetry in the CGLe [263]. Inclusion of higher order terms, such as a quintic term $\delta|A|^4A$ eliminates this family of solutions [68]. So, the family is structurally unstable, and the hidden symmetry appears specific to the cubic CGLe. In the stationary case, the existence of the solitory solution and more complicated solutions can be inferred by an application of the counting argument associated with the reflection symmetry [14].

4.1.3 Stokes solutions and their stability

The global phase invariance implies that the CGLe has nonlinear plane wave solutions of the form

$$A(x,t) = R_0 \exp(i(qx - \omega t))\,, \tag{72}$$

where $R_0^2 = \mu - q^2$ is the square of the amplitude, $\omega = \mu\beta + (\alpha-\beta)q^2$ is the frequency, and $q \in \mathbb{R}$ with $q^2 \leq \mu$ is the wavenumber. They are called Stokes solutions [3] and are parametrized by the wavenumber q. The two limit cases of interest to us are highlighted on figure 8: a plane wave of wavenumber $\mu^{1/2}$ and of vanishing amplitude (case I), and the wave with zero wavenumber and maximum amplitude μ (case II). In case II, the solution oscillates uniformly in space; we call it the homogeneously oscillating state (HOS).

For the infinite system, the Benjamin-Feir-Newell [190] criterion states that all plane wave solutions are unstable with respect to long wavelength perturbations, *i.e.*, of wavenumber $k \to 0$) if $1 + \alpha\beta < 0$. If $1 + \alpha\beta > 0$, we have to consider the Eckhaus stability criterion

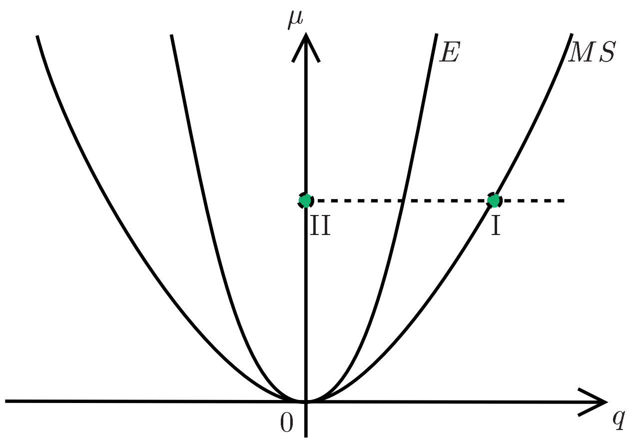

Figure 8: Marginal stability curve (MS) and Eckhaus instability curve (E) defining regions where plane waves solutions exist in the CGLe (inside (MS)), and are stable when $1+\alpha\beta>0$ (inside (E)). Case I corresponds to the wave of maximal possible wavenumber and Case II to the wave with $q=0$ and the maximal amplitude.

which states that only a band of wavenumbers are stable against long wavelength perturbations:

$$q^2 < q_{\mathrm{E}}^2 \equiv \frac{(1+\alpha\beta)\mu}{3+\alpha\beta+2\beta^2}\,. \tag{73}$$

For a finite periodic system the wavenumbers for both the original states and the perturbations are quantized. In this context, the above criteria were re-examined by Matkowsky and Volpert using linear stability analysis [174].

4.1.4 Low-dimensional behavior of the CGLe

The CGLe describes a dynamical system with infinitely many degrees of freedom. But in either experiments or numerical simulations, only a finite number of patterns play a role in the long-time dynamics. For the CGLe in a periodic box, a global attracting set exist towards which all the solutions approach in a finite time. An upper bound on the number of Fourier modes needed to give a complete knowledge of the asymptotic dynamics is derived in ref. [70]. The rest of the infinitely many modes are determined by geometric constraints that define the finite-dimensional inertial manifold in the phase space. Thus, the global attractor which lies on the inertial manifold also has a finite dimension. By estimating the Lyapunov exponents on the asymptotic trajectory, similar result was also claimed in ref. [96]. In the even solution space, the magnitude of the Mth mode of the global attractor decays faster than any algebraic order of M^{-1} [67].

Though the above analytic results provide a rigorous justification for simulating the CGLe dynamics with finite Gälerkin truncations, these estimated bounds on the number of effective modes are usually much higher than what is needed for actual numerical calculations. In practice, we always try to use the smallest number of modes, sufficient to capture the dynamics of interest. Near the onset of chaotic behavior, just a few modes are important and enough to give a complete description of bifurcation sequences [67, 165]. In the chaotic region, a common approach to select the optimal basis is the Karhunen-Loeve or proper orthogonal decomposition (POD) which orders the orthogonal linear basis according to their relative importance [212] by checking the 2-point correlation matrix on the strange attractor. This method does not utilize geometrical information about the layout of inertial manifold, and is inadequate for our purposes.

In a periodic box, we can clearly see how the destabilization of low wavenumber modes leads to spatiotemporal chaos. When the size L is small, homogeneous oscillatory state (HOS) is stable. The first instability generates stationary modulated amplitude waves (MAWs). They partially break the space translational symmetry but retain the parity. The ensueing pitchpork bifurcation breaks the parity of $|A|$ and sets the whole profile moving. As the system size increases further, spatiotemporal chaos arises and both the amplitude and phase of A fluctuate irregularly. Bifurcations in the even solution space have been studied in great detail [67, 165]. Similarly to the Lorenz attractor [236], the first strange attractor is generated through a homoclinic explosion [165].

4.1.5 Phase chaos versus defect chaos

In the infinite domain all the plane waves become unstable above the Benjamin-Feir (BF) line ($1 + \alpha\beta < 0$) [22], and the system becomes chaotic. There are two types of chaos in the chaotic region: phase chaos and defect (or amplitude) chaos. In the phase chaos, the amplitude of A is bounded away from zero, while in the defect chaos $|A|$ reaches zero at isolated space-time points. When $|A(x,t)| = 0$, we say that a defect forms; at the defect point the phase of A is not defined. The Bekki-Nozaki solutions are believed to play an important role in the defect chaos. Two characteristics can be used to distinguish phase chaos and defect chaos [254, 185, 256]: the defect density n_d which is the space-time average of the number of defects that appear in the system, and the phase winding number

$$\nu = \frac{1}{2\pi}\int_0^L \partial_x \phi(x,t)\, dx$$

which represents the phase change of A over the interval. In the defect chaotic region, $n_d \neq 0$ and $\nu = 0$ but in the phase chaotic one $n_d = 0$ and $\nu \neq 0$. There exists a line in the α, β parameter space below which only defect chaos is present [229] (see figure 9). The line consists of two parts: L_1 and L_3 (we use the notation of ref. [229]). Across L_1 the transition is continuous [229, 77]. Near L_3, there is a bichaotic region, where both the phase chaos and the defect chaos are metastable and they may transform to each other by finite-amplitude perturbations. The L_1 line can be continued to L_2 which crosses the BF line. A spatiotemporal intermittency region [35] lies below the L_2 line where the metastable states are plane waves and defect chaos.

Near the BF line in the phase chaotic region, the states result from a Hopf bifurction of the HOS when the long-wavelength components become linearly unstable. As the interaction between different modes is very weak, each mode can be viewed as an independent oscillator with the amplitude entrained to the phase (see sect. 5.1 in Chapter 5), and thus

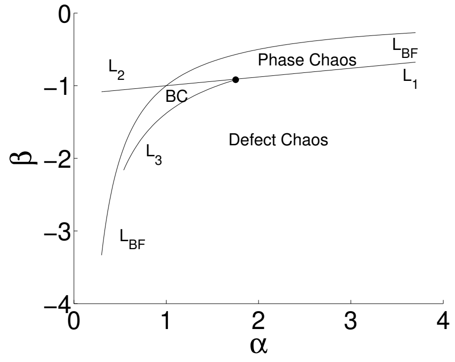

Figure 9: Phase diagram of the CGLe. The line L_{BF} is the locus of the Benjamin-Feir instability. L_1, L_2 and L_3 intersect at the point C^*. Below L_1 and L_3, only defect chaos is observed. The region enclosed by L_2, L_3 and L_{BF} is a bichaotic region (marked BC). Note that L_2 crosses L_{BF}.

phase equations can be developed to describe the evolution of the system [154]. The most commonly used one is the Kuramoto-Sivashinsky equation (KSe) [155, 232]. In the defect chaos region, the interaction between modes are so strong that $|A|$ is brought down to zero at discrete space-time points where the winding number changes through phase-slip process. In this case, the defect dynamics sets in and phase equation fails [222].

4.2 Coherent structures and MAWs

In extended systems, chaotic states are usually a juxtapostion of patches of regular patterns called "coherent structures" (CS) [263]. The CS play a very important role in the study of pattern formation and dynamical properties of the CGLe. In the laminar case, the CS includes uniform states, plane waves, pulses, fronts, holes. In the chaotic case, the overall pattern consists of near-regular patches connected by localized defects or interfaces. After doing the following substitution in (70),

$$A(x,t) \to A(x-ct,t)e^{i(kx-\omega t)}\,,$$

we get

$$A_t = (\mu - k^2 + i\omega)A + (c+2ik)A_x + (1+i\alpha)A_{xx} - (1+i\beta)|A|^2 A\,. \tag{74}$$

The coherent structures we will discuss below are the steady solutions of (74), *i.e.*, $A_t = 0$. There exists a similarity transformation which maps steady states to each other for different $\alpha\,,\beta$ values in the parameter space along the constant C-curve

$$C = \frac{\alpha - \beta}{1 + \alpha\beta}\,.$$

$k\,,c\,,A$ and ω have to change accordingly during the process while the shape of the magnitude profile of A does not change.

In the steady equation, if we use polar coordinates,

$$A(x,t) = R(x)e^{i\phi(x)}\,,$$

a 3-D nonlinear dynamical system is obtained [263]

$$
\begin{aligned}
R_x &= \psi \\
\psi_x &= R\kappa^2 + \frac{1+\alpha\beta}{1+\alpha^2}R^3 + (2kR - \frac{c\alpha}{1+\alpha^2})\kappa - \frac{c}{1+\alpha^2}\psi + \frac{k^2+\alpha^2k^2-\mu-\alpha\omega}{1+\alpha^2}R \\
\kappa_x &= \frac{\beta-\alpha}{1+\alpha^2}R^2 + \frac{\alpha\mu-\omega}{1+\alpha^2}(\frac{c\alpha}{1+\alpha^2} - 2k)\frac{\psi}{R} - \frac{2\kappa\psi}{R} - \frac{c}{1+\alpha^2}\kappa\,, \qquad (75)
\end{aligned}
$$

where $\psi = R_x$ is the gradient of R and $\kappa = \phi_x$ is the local wavenumber. By redefining ω and κ, the parameter k can be set to zero. There are essentially two free parameters: the frequency ω and the group velocity c. when $c = 0$, (75) becomes an equation for the stationary solution of the CGLe and is invariant under the transformation $(R, \psi, \kappa, x) \to (R, -\psi, -\kappa, -x)$.

The equilibrium points of (75) are plane waves described in sect. 4.1.3. The homoclinic [257] and heteroclinic [263] connections between equilibria correspond to localized coherent structures. The Nozaki-Bekki solutions [15] belong to this category; they connect asymptotic plane waves with different wavenumbers. In large domain numerical simulations, near-coherent structures are frequently observed in the intermittency or chaotic regimes [229, 261, 263, 35, 4, 258, 259, 196, 15] and play an essential role in the pattern formation process.

Recent numerical studies reveal another kind of coherent structure: modulated amplitude waves (MAWs) for the CGLe [30]. They correspond to limit cycles of (75). When $c = 0$, MAWs are stationary. The formation of MAWs is the first instability encountered when a plane wave state crosses the Eckhaus or Benjamin-Feir stability line. The MAW structure is frequently observed in experiments [137, 95], and is considered a key to interpretation of patterns and bifurcations exhibited during the system's transition to spatiotemporal chaos [28, 27, 30].

In the following, we reformulate the equation for steady solutions, and prove the existence of MAWs for case I and II. The stability analysis indicates that the MAWs arising in case I are unstable but the MAWs in case II are stable. By comparing with numerical calculations, we find that the later ones are indeed the stationary waves observed after the first bifurcation.

4.3 Reformulation of the problem

Since we are only interested in the steady solutions of the CGLe, we substitute the ansatz

$$A(x,t) = R(x)\exp(i\phi(x) - i\omega t), \qquad (R,\phi) \in \mathbb{R}^2 \qquad (76)$$

into (70). We then have

$$
\begin{aligned}
(1+\alpha^2)G_x &= K \equiv (\beta-\alpha)R^4 - (\omega-\mu\alpha)R^2 \qquad (77)\\
(1+\alpha^2)G^2 &= M \equiv (1+\alpha^2)R^3R_{xx} + (\alpha\omega+\mu)R^4 - (1+\alpha\beta)R^6\,. \qquad (78)
\end{aligned}
$$

where $G \equiv \phi_x R^2$ is reminiscent of “angular momentum”. Note that if $\alpha = \beta$, this “angular momentum” is conserved — it is constant in space — provided that $\omega = \mu\alpha$. In that case,

(78) can be solved in terms of elliptic functions [162]. We will only consider the case $\alpha \neq \beta$ in the following. Equations (77) and (78) are invariant under $(G, x, R) \to (-G, -x, \pm R)$. Note that for plane waves, $K = 0$ and G is a constant. If K is not always zero, differentiating (78) and dividing the result by (77) gives

$$2G = M_x/K \,, \tag{79}$$

and by (78)

$$M = \frac{1+\alpha^2}{4}\frac{M_x^2}{K^2} \,. \tag{80}$$

Furthermore, we can factorize R^2 from M_x and K and write $M_x = R^2 N$ and $K = R^2 P$, where

$$\begin{aligned} N &\equiv (1+\alpha^2)\frac{1}{2}(R^2)_{xxx} + (\alpha\omega+\mu)2(R^2)_x - (1+\alpha\beta)3R^2(R^2)_x \\ P &\equiv (\beta-\alpha)R^2 - (\omega-\mu\alpha) \,. \end{aligned} \tag{81}$$

The last relation can be used to express R^2 in terms of P:

$$R^2 = \frac{(\omega-\mu\alpha)+P}{\beta-\alpha} = e + dP = R_0^2 + \frac{P}{\beta-\alpha} \,, \tag{82}$$

where $d \equiv 1/(\beta-\alpha)$ and $e \equiv (\omega-\mu\alpha)/(\beta-\alpha)$.

Note that $e = R_0^2$ is the square of the homogeneous amplitude $R_0(q,\omega)$ of the Stokes plane wave solution (72) of frequency ω and wavevector $q(\omega)$. P then appears as the modulation of the amplitude squared with respect to the Stokes solution, and so it is an appropriate variable to describe a MAW.

Substituting K and M_x into (80), we have

$$\frac{1+\alpha^2}{4}\frac{N^2}{P^2} = M \,. \tag{83}$$

If $P \neq 0$ (83) is equivalent to (77) and (78). It is easy to check that if we regard (79) as a definition of G, and use K, M, N, P expressed in terms of R, equation (77) and (78) will be recovered as a result of (80) and (83). Differentiating both sides of (83) results in

$$\frac{1+\alpha^2}{2}(PN_x - NP_x) = R^2P^3 \,. \tag{84}$$

In this step we have extended the solution set of (83), because as we integrate (84) back, we get

$$\frac{1+\alpha^2}{4}\frac{N^2}{P^2} = M + \mathcal{C} \,, \tag{85}$$

where $\mathcal{C}$ is an integration constant. Only for $\mathcal{C} = 0$ a solution of (84) is a solution of (83). For this reason, when obtaining solutions of (84), we have to check the *consistency condition*

$$\frac{1+\alpha^2}{4}\frac{N^2}{P^2} - M = 0 \tag{86}$$

to make sure that we have a solution of (83), thus a solution of (77) and (78). Note that if K vanishes identically we have to go back to (77) and (78), since in that case (83) is not well defined. Let us rewrite N in terms of P:

$$N = \frac{2}{1+\alpha^2}\left(aP_{xxx} + bP_x + cPP_x\right) , \tag{87}$$

where a, b, c are constants

$$\begin{aligned} a &\equiv \frac{(1+\alpha^2)^2}{4(\beta-\alpha)} \\ b &\equiv \frac{1+\alpha^2}{2}\left(\frac{2(\alpha\omega+\mu)}{\beta-\alpha} - \frac{3(1+\alpha\beta)(\omega-\mu\alpha)}{(\beta-\alpha)^2}\right) \\ c &\equiv -\frac{3(1+\alpha\beta)(1+\alpha^2)}{2(\beta-\alpha)^2} . \end{aligned} \tag{88}$$

We use (87) and (82) to rewrite (84) using only P and its spatial derivatives:

$$P(aP_{xxx} + bP_x + cPP_x)_x - P_x(aP_{xxx} + bP_x + cPP_x) = (dP+e)P^3 \tag{89}$$

Note that this equation contains even numbers of derivatives of P in each term on the left hand side, and also that the powers of P increase while the derivatives decrease. We now rewrite the equation in a form which takes advantage of this structure. For example, the following equation is equivalent to (89) for any real λ:

$$\begin{aligned} P(aP_{xxx} + bP_x + (c+\lambda)PP_x)_x - P_x(aP_{xxx} + bP_x + (c+\lambda)PP_x) \\ = P^2(\lambda P_{xx} + dP^2 + eP) , \end{aligned}$$

or, put in another form and introducing another real parameter k:

$$\left(\frac{(aP_{xx} + bP + \frac{c+\lambda}{2}P^2)_x}{P}\right)_x = \lambda P_{xx} + dP^2 + \tilde{e}P + \frac{a}{\lambda}kP ,$$

where we have written $\tilde{e} + \frac{a}{\lambda}k = e$.

In this equation, we have three free parameters: besides ω, introduced by the ansatz (76) as the carrier frequency of the solution, we have introduced free parameters λ and k. We now fix λ by imposing the condition

$$\frac{a}{\lambda} = \frac{b}{\tilde{e}} = \frac{c+\lambda}{2d} , \tag{90}$$

which allows us to write the equation in a more suggestive form:

$$\left(\frac{(\lambda P_{xx} + dP^2 + \tilde{e}P)_x}{P}\right)_x = \frac{\lambda}{a}(\lambda P_{xx} + dP^2 + \tilde{e}P) + kP ,$$

or more concisely,

$$\left(\frac{\tilde{M}_x}{P}\right)_x = \frac{\lambda}{a}\tilde{M} + kP , \qquad \text{where } \tilde{M} \equiv \lambda P_{xx} + dP^2 + \tilde{e}P . \tag{91}$$

This equation will lead to the 4-D ODE of section 4.4.

λ is determined by (90):

$$\lambda^2 + c\lambda - 2ad = 0\,. \tag{92}$$

The discriminant of (92) is

$$\begin{aligned}\Delta &= c^2 + 8ad \\ &= \left(\frac{1+\alpha^2}{2(\beta-\alpha)}\right)^2 \left(\frac{9(1+\alpha\beta)^2}{(\beta-\alpha)^2} + 8\right)\,.\end{aligned}$$

So $\Delta > 0$ for any real values of α and β, and the quadratic equation (92) always has two real roots

$$\lambda = \frac{3(1+\alpha\beta)(1+\alpha^2)}{4\,(\beta-\alpha)^2} \pm \frac{1+\alpha^2}{4(\beta-\alpha)^2}\sqrt{9(1+\alpha\beta)^2 + 8(\beta-\alpha)^2} \tag{93}$$

Note that λ is a function of α and β only. In some applications [207], the two values of λ correspond to two distinct solutions of the CGLe. In our case, λ is an intermediate variable used in the derivation and the proofs, but our solutions to the CGLe do not distinguish the two values of λ.

4.4 4-D dynamical system and the existence of periodic solutions

Let us take τ as the spatial variable, $P = P(\tau)$ in (81), and rewrite (91) as a system of first order equations in τ. With $\tilde{N} = \tilde{M}_\tau / P$ and $Q = P_\tau$, from (91) we have

$$\left\{\begin{array}{lcl} \dot{\tilde{M}} &=& \tilde{N}P \\ \dot{\tilde{N}} &=& \frac{\lambda}{a}\tilde{M} + kP \\ \dot{P} &=& Q \\ \dot{Q} &=& \frac{1}{\lambda}(\tilde{M} - dP^2 - \tilde{e}P) \end{array}\right. , \tag{94}$$

where the dot represents the derivative with respect to the spatial variable τ.

It is easy to check that $P \equiv 0$ is a solution of the original equations (77) and (78), corresponding to the plane wave solution of the CGLe with frequency ω. We will study the behavior near $P = 0$ and prove the existence of periodic solutions for small P. In the CGLe, this corresponds to a weakly modulated amplitude wave which bifurcates from a plane wave solution. If $P \sim \epsilon$, where ϵ is a small parameter, so are $\tilde{M}, \tilde{N}, Q$ by their definitions. Write

$$(\tilde{M}, \tilde{N}, P, Q) = (\epsilon x, \epsilon y, \epsilon z, \epsilon w)$$

and set $k = k_1 + \epsilon k_2$. Substituting these into the 4-D system, we have

$$\frac{d}{d\tau}\begin{pmatrix} x \\ y \\ z \\ w \end{pmatrix} = A \begin{pmatrix} x \\ y \\ z \\ w \end{pmatrix} + \epsilon \begin{pmatrix} y\,z \\ k_2\,z \\ 0 \\ -\frac{d}{\lambda}z^2 \end{pmatrix}, \text{ where } A = \begin{pmatrix} 0 & 0 & 0 & 0 \\ \frac{\lambda}{a} & 0 & k_1 & 0 \\ 0 & 0 & 0 & 1 \\ \frac{1}{\lambda} & 0 & \frac{-\tilde{e}}{\lambda} & 0 \end{pmatrix}.$$

The linear part A describes the behavior of the system in the neighborhood of the trivial fixed point $(0,0,0,0)$. Note that the system is invariant under $(t,y,w) \to -(t,y,w)$. We will use this property to simplify our analysis. Moreover, this system defines an incompressible flow since $\nabla \cdot \vec{X} = 0$, where $\vec{X} = (x,y,z,w)$. It follows from (85) that the system has one integration constant $\mathcal{C}$. This constant induces a foliation of the phase space into three-dimensional manifolds. Physical solutions, i.e., the solutions of the original CGLe, are restricted to $\mathcal{C} = 0$, the manifold that satisfies the *consistency condition* (86).

These properties strongly restrict the possible distributions of eigenvalues of A. We restrict our analysis to the case $\tilde{e}/\lambda > 0$. In that case, A has eigenvalues $\{0, 0, i\omega_1, -i\omega_1\}$ with $\omega_1 = \sqrt{\tilde{e}/\lambda}$, and periodic solutions or MAWs can exist, as we will prove in the following. The evolution of the system respects the constant $\mathcal{C}$ foliation: if the solution is on a constant $\mathcal{C}$ manifold at initial time, it remains there for any later time.

We now discuss the condition $\tilde{e}/\lambda > 0$ in terms of an instability of the underlying plane wave. We can rewrite $\tilde{e}/\lambda$ using (88) and (90). Assuming that the solution we are searching for is close to a plane wave, we can use the wavenumber q instead of the frequency ω, using the dispersion relation (72) for plane waves:

$$\begin{aligned} \frac{\tilde{e}}{\lambda} = \frac{b}{a} &= \frac{2}{1+\alpha^2}\left[2(\alpha\omega + \mu) - \frac{3(1+\alpha\beta)(\omega - \mu\alpha)}{\beta - \alpha}\right] \\ &= \frac{2}{1+\alpha^2}\left[(3 + \alpha\beta + 2\alpha^2)q^2 - (1+\alpha\beta)\mu\right] . \end{aligned} \tag{95}$$

If we write

$$q_{\mathrm{M}}^2 \equiv \frac{(1+\alpha\beta)\mu}{3 + \alpha\beta + 2\alpha^2} , \tag{96}$$

we have

$$\frac{\tilde{e}}{\lambda} > 0 \quad \Leftrightarrow \quad \left| \begin{array}{rll} q^2 > q_{\mathrm{M}}^2 & \text{if} & (1+\alpha\beta) > 0 \\ q^2 < q_{\mathrm{M}}^2 & \text{if} & (1+\alpha\beta) < -2(1+\alpha^2) \\ \forall q \in [-\sqrt{\mu}, \sqrt{\mu}] & \text{if} & -2(1+\alpha^2) < 1 + \alpha\beta < 0 \end{array} \right. . \tag{97}$$

The corresponding regions are illustrated on Fig. 10. Note that $q_{\mathrm{M}}(\alpha,\beta,\mu) = q_{\mathrm{E}}(\beta,\alpha,\mu)$. If $|\alpha| = |\beta|$, the positivity of $\tilde{e}/\lambda$ is assured when the corresponding plane wave is Eckhaus unstable. If $|\alpha| \neq |\beta|$, the positivity does not coincide anymore with the Eckhaus criterion; this is not surprising considering that we do not restrict our analysis to long wavelength perturbations of plane waves, but that the solutions we are seeking may have any wavenumber.

In the following we distinguish two cases. In the first case eigenvalue 0 has a simple elementary divisor, *i.e.*, has two distinct eigenvectors [113]. This coincides with case I: the MAW solution bifurcates from the $A = 0$ state, with $\omega \sim \mu\alpha$ and hence $\tilde{e}/\lambda \sim 4\mu > 0$, for $\mu > 0$. In the second case, eigenvalue 0 has only one eigenvector. This coincides with case II: the MAW is superimposed over a plane wave with $\omega \simeq \mu\beta$, so $q \simeq 0$, and

$$\frac{\tilde{e}}{\lambda} \simeq -\frac{2\mu(1+\alpha\beta)}{1+\alpha^2} > 0,$$

where the positivity is insured if the system is Benjamin-Feir-Newell unstable, $(1+\alpha\beta) < 0$.

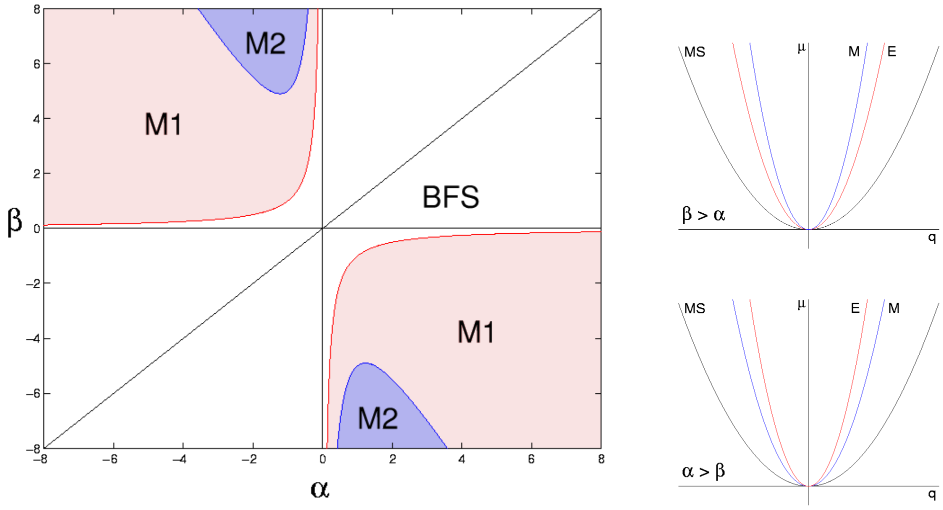

Figure 10: Left: wavenumber distribution of stationary MAWs in the (α, β) plane. In (BFS), MAWs exist if $q^2 > q_{\rm M}^2$. In (M1), MAWs exist $\forall q$. In (M2), MAWs exist if $q^2 < q_{\rm M}^2$. Right: regions of existence of MAWs in the (q, μ) plane in the Benjamin-Feir-Newell stable regime ((BFS) region). (MS) is the marginal stability curve, (E) is the Eckhaus instability curve and (M) is existence curve defined by (96). Stationary MAWs exist outside (M).

In terms of $\tilde{M}, \tilde{N}, P, Q$, the *consistency condition* (86) can be written as

$$(1+\alpha^2)M = \left(\frac{a}{\lambda}\tilde{N} - \lambda Q\right)^2 \tag{98}$$

where in new variables

$$\begin{aligned} M \quad = \quad & \frac{d(1+\alpha^2)}{2\lambda}(d\,P+e)(\tilde{M} - d\,P^2 - \tilde{e}\,P) - \frac{d^2(1+\alpha^2)}{4}Q^2 + \\ & (\alpha\omega + \mu)(d\,P+e)^2 - (1+\alpha\,\beta)(d\,P+e)^3\,. \end{aligned}$$

Recalling (78), we may express G by

$$G = \frac{\frac{a}{\lambda}\tilde{N} - \lambda Q}{1+\alpha^2}\,. \tag{99}$$

Here we are allowed to fix the sign of the right hand side expression because of the $(G, x) \mapsto (-G, -x)$ reflection symmetry of (77) and (78).

4.4.1 Case I

We want the eigenvalue 0 to have non-degenerate eigenvectors, for this, we set

$$\frac{\frac{\lambda}{a}}{\frac{1}{\lambda}} = \frac{k_1}{-\frac{\tilde{e}}{\lambda}}\,, \qquad i.e.,\ k_1 = -\frac{\lambda\tilde{e}}{a}\,.$$

Consequently, we have

$$e = \tilde{e} + \frac{a}{\lambda}k = \frac{\epsilon a}{\lambda}k_2\,. \tag{100}$$

Notice that $e \sim 0$ to the zeroth order, so $R_0 \sim 0$ and $\omega \sim \mu\alpha$, which means that the solution to be considered bifurcates from the zero solution $A = 0$, corresponding to a plane wave around the marginal stability curve, with wavenumber $q \sim \pm\mu^{1/2}$. This solution is therefore outside the Eckhaus stability region when $1 + \alpha\beta > 0$.

The four eigenvectors of A are:

$$\begin{pmatrix} 0 \\ 1 \\ 0 \\ 0 \end{pmatrix} \quad \begin{pmatrix} \tilde{e} \\ 0 \\ 1 \\ 0 \end{pmatrix} \quad \begin{pmatrix} 0 \\ -ik_1\omega_1^{-1} \\ 1 \\ i\omega_1 \end{pmatrix} \quad \begin{pmatrix} 0 \\ ik_1\omega_1^{-1} \\ 1 \\ -i\omega_1 \end{pmatrix}.$$

Let

$$D = \begin{pmatrix} 0 & \tilde{e} & 0 & 0 \\ 1 & 0 & 0 & \frac{\lambda^2}{a} \\ 0 & 1 & 1 & 0 \\ 0 & 0 & 0 & 1 \end{pmatrix}, \qquad D^{-1} = \begin{pmatrix} 0 & 1 & 0 & -a^{-1}\lambda^2 \\ \tilde{e}^{-1} & 0 & 0 & 0 \\ -\tilde{e}^{-1} & 0 & 1 & 0 \\ 0 & 0 & 0 & 1 \end{pmatrix},$$

and $\vec{\tilde{X}} \equiv (\tilde{x}, \tilde{y}, \tilde{z}, \tilde{w}) = D^{-1}\vec{X}$. The dynamical equations for the new variables become

$$\frac{d}{d\tau}\vec{\tilde{X}} = M(\omega_1)\vec{\tilde{X}} + \epsilon \begin{pmatrix} k_2(\tilde{y}+\tilde{z}) + \frac{\lambda d}{a}(\tilde{y}+\tilde{z})^2 \\ \frac{1}{\tilde{e}}(\tilde{x} + \frac{\lambda^2}{a}\tilde{w})(\tilde{y}+\tilde{z}) \\ -\frac{1}{\tilde{e}}(\tilde{x} + \frac{\lambda^2}{a}\tilde{w})(\tilde{y}+\tilde{z}) \\ -\frac{d}{\lambda}(\tilde{y}+\tilde{z})^2 \end{pmatrix},$$

where

$$M(\omega_1) = D^{-1}AD = \begin{pmatrix} 0 & 0 & 0 & 0 \\ 0 & 0 & 0 & 0 \\ 0 & 0 & 0 & 1 \\ 0 & 0 & -\omega_1^2 & 0 \end{pmatrix}.$$

The angular frequency of the solution Ω should be close to ω_1, $\Omega^2 = \omega_1^2 + \epsilon\gamma$, with the shift γ to be determined later. Next, we change variables to:

$$\left\{ \begin{array}{rcl} \tilde{x} & = & x_1 \\ \tilde{y} & = & x_2 \\ \tilde{z} & = & z_1 \sin\Omega\tau + z_2 \cos\Omega\tau \\ \tilde{w} & = & \Omega z_1 \cos\Omega\tau - \Omega z_2 \sin\Omega\tau \end{array} \right. \tag{101}$$

The 4-D system of equations then takes form:

$$
\begin{aligned}
\dot{x_1} &= \epsilon\left[k_2(x_2+z_1\sin\Omega\tau+z_2\cos\Omega\tau)+\frac{\lambda d}{a}(x_2+z_1\sin\Omega\tau+z_2\cos\Omega\tau)^2\right]\\
\dot{x_2} &= \frac{\epsilon}{\tilde{e}}\left[x_1+\frac{\Omega\lambda^2}{a}(z_1\cos\Omega\tau-z_2\sin\Omega\tau)\right](x_2+z_1\sin\Omega\tau+z_2\cos\Omega\tau)\\
\dot{z_1} &= \frac{\epsilon}{\Omega}\left[-\frac{d}{\lambda}(x_2+z_1\sin\Omega\tau+z_2\cos\Omega\tau)^2\cos\Omega\tau\right.\\
&\quad+\gamma(z_1\sin\Omega\tau+z_2\cos\Omega\tau)\cos\Omega\tau\\
&\quad\left.-\frac{\Omega}{\tilde{e}}\left(x_1+\frac{\Omega\lambda^2}{a}(z_1\cos\Omega\tau-z_2\sin\Omega\tau)\right)(x_2+z_1\sin\Omega\tau+z_2\cos\Omega\tau)\sin\Omega\tau\right]\\
\dot{z_2} &= \frac{\epsilon}{\Omega}\left[\frac{d}{\lambda}(x_2+z_1\sin\Omega\tau+z_2\cos\Omega\tau)^2\sin\Omega\tau\right.\\
&\quad-\gamma(z_1\sin\Omega\tau+z_2\cos\Omega\tau)\sin\Omega\tau\\
&\quad\left.-\frac{\Omega}{\tilde{e}}\left(x_1+\frac{\Omega\lambda^2}{a}(z_1\cos\Omega\tau-z_2\sin\Omega\tau)\right)(x_2+z_1\sin\Omega\tau+z_2\cos\Omega\tau)\cos\Omega\tau\right]
\end{aligned}
\tag{102}
$$

The proof of the existence of weak MAWs close to $P=0$ relies on a series of theorems from J. Hale's monograph [113]. We reproduce the relevant theorems in appendix **??**, and refer to them as the need arises.

Note that the transformation $(\tau,x_1,x_2,z_1,z_2)\to(-\tau,-x_1,x_2,-z_1,z_2)$ leaves the system (102) invariant. So, by definition C.0.1 of appendix **??** the system has the property E with respect to Q, with

$$Q=\mathrm{diag}(-1,1,-1,1)\,.$$

As we are interested only in the solutions with definite parity, we may start the iteration with the vector

$$\vec{X_0}=(0,a_2,0,a_4)\,.$$

According to Theorem C.0.4, our solution $z(\tau,\vec{X_0},\epsilon)$ has the property

$$Qz(-\tau,\vec{X_0},\epsilon)=z(\tau,\vec{X_0},\epsilon)\,,$$

which means that our solutions are either symmetric or antisymmetric. According to Theorem C.0.5, the second and the fourth determining equations are always zero for this starting vector. For the first and the third determining equations, the zeroth order solution of $\vec{\tilde{X}}$, *i.e.*, $\vec{X_0}$, may be substituted in, and we get

$$
\begin{aligned}
k_2a_2+\frac{\lambda d}{a}(a_2^2+\frac{1}{2}a_4^2) &= 0 \qquad (103)\\
\frac{\gamma}{2\Omega}a_4+\frac{\lambda^2\Omega a_2a_4}{2a\tilde{e}}-\frac{d}{\lambda\Omega}a_2a_4 &= 0\,. \qquad (104)
\end{aligned}
$$

From (104), we have two possibilities: either $a_4=0$ or

$$\gamma+a_2\left(\frac{\lambda^2\Omega^2}{a\tilde{e}}-\frac{2d}{\lambda}\right)=0\,. \tag{105}$$

When $a_4 = 0$, using $\vec{X}_0 = (0, a_2, 0, 0)$ in (102) leads to a trivial constant solution. In the following, we consider only the second case (105). We can solve (103) and (105) for γ and a_4 and prove that the system (102) has periodic solutions. Note that we have three free parameters ϵ, a_2, k_2. But as we will see further, ϵ and a_2 are always combined as ϵa_2 in the first approximation controlling the amplitude and the period of the solution, and the combination will therefore be regarded here as one single free parameter. For general periodic solutions without parity, a_2 can be interpreted as a phase control parameter, *i.e.*, a parameter giving the initial location on the periodic orbit at $\tau = \tau_0$. Here, because we only consider symmetric solutions, the translational symmetry of the autonomous system is broken, and that is the reason why ϵ and a_2 combine into a single parameter. The remaining parameter k_2 can be chosen freely, for example as to satisfy the *consistency condition* (98), which, when the zeroth order solution is substituted, becomes at order (ϵ^2):

$$-\frac{d^2}{4}\,\Omega^2\, a_4^2 + \mu\left(da_2 + \frac{k_2 a}{\lambda}\right)^2 = 0\,. \tag{106}$$

At zeroth order, $\Omega^2 = \omega_1^2 = 4\mu$ and $\tilde{e} = 4\mu\lambda$. Solving the system of equations (103), (105) and (106), we get

$$\left\{\begin{array}{rcl} k_2 & = - & \frac{3\lambda}{a} da_2 \\ \gamma & = & \frac{c}{a} a_2 \\ a_4 & = & \pm 2a_2 \end{array}\right. .$$

We can write out the Jacobian for those three equations explicitly:

$$J = \begin{pmatrix} a_2 & 0 & \frac{\lambda d}{a} a_4 \\ 0 & 1 & 0 \\ \frac{2\mu a}{\lambda}(da_2 + \frac{k_2 a}{\lambda}) & 0 & -\frac{d^2}{2}\Omega^2 a_4 \end{pmatrix}.$$

The determinant of this Jacobian is

$$\det J = \frac{1}{2} d^2 \Omega^2 a_2 a_4 \neq 0\,, \qquad a_2 \neq 0\,.$$

We now invoke theorem C.0.2, reproduced in Appendix A, and conclude our proof that system (77) and (78) has periodic solutions near $P = 0$. We shall show that in this case the periodic solutions contain defects and give their approximate analytic expressions in section 4.5.

4.4.2 Case II

Eigenvalue 0 has only one eigenvector. In this case, we assume that $\frac{\lambda}{a}\tilde{e} + k_1 \neq 0$ to the zeroth order in ϵ, so without loss of generality we can choose $k_2 = 0$. Then $\frac{\lambda}{a} e = \frac{\lambda}{a}\tilde{e} + k_1$. Implementing the transformation $\vec{X} = D\vec{\tilde{X}}$ with

$$D = \begin{pmatrix} 0 & \tilde{e} & 0 & 0 \\ 1 & 0 & 0 & -k_1\omega_1^{-2} \\ 0 & 1 & 1 & 0 \\ 0 & 0 & 0 & 1 \end{pmatrix}$$

we have

$$\frac{d}{d\tau}\vec{\tilde{X}} = M(\omega_1)\vec{\tilde{X}} + \epsilon \begin{pmatrix} -\frac{d}{\tilde{e}}k_1(\tilde{y}+\tilde{z})^2 \\ \frac{1}{\tilde{e}}(\tilde{x}-k_1\frac{\lambda}{\tilde{e}}\tilde{w})(\tilde{y}+\tilde{z}) \\ -\frac{1}{\tilde{e}}(\tilde{x}-k_1\frac{\lambda}{\tilde{e}}\tilde{w})(\tilde{y}+\tilde{z}) \\ -\frac{d}{\lambda}(\tilde{y}+\tilde{z})^2 \end{pmatrix},$$

where

$$M(\omega_1) = D^{-1}AD = \begin{pmatrix} 0 & \frac{\lambda e}{a} & 0 & 0 \\ 0 & 0 & 0 & 0 \\ 0 & 0 & 0 & 1 \\ 0 & 0 & -\omega_1^2 & 0 \end{pmatrix}.$$

As in case I, let $\Omega^2 = \omega_1^2 + \epsilon\gamma$ and perform the same transformation (101) into variables x_1, x_2, z_1, z_2. We then obtain a 4-D system similar to (102). However, in the equation for $\dot{x_1}$, there is an ϵ-free term. In order to use the successive approximation method, further transformations are required. Let $\rho \in \mathbb{R}$ such that $\rho^2 = \epsilon$. With the transformation $x_2 \to \rho x_2, \epsilon \to \rho^2$ we recover the standard form

$$\begin{aligned}
\dot{x_1} &= \frac{\rho\lambda e}{a}x_2 - \rho^2 k_1 \frac{d}{\tilde{e}}(\rho x_2 + z_1 \sin\Omega\tau + z_2 \cos\Omega\tau)^2 \\
\dot{x_2} &= \frac{\rho}{\tilde{e}}\left[x_1 - k_1\frac{\Omega\lambda}{\tilde{e}}(z_1 \cos\Omega\tau - z_2\sin\Omega\tau)\right](\rho x_2 + z_1\sin\Omega\tau + z_2\cos\Omega\tau) \\
\dot{z_1} &= \frac{\rho^2}{\Omega}\left[\frac{-d}{\lambda}(\rho x_2 + z_1\sin\Omega\tau + z_2\cos\Omega\tau)^2\cos\Omega\tau \right. && (107) \\
& +\gamma(z_1\sin\Omega\tau + z_2\cos\Omega\tau)\cos\Omega\tau && (108) \\
& \left. -\frac{\Omega}{\tilde{e}}\left(x_1 - \frac{\Omega\lambda}{\tilde{e}}k_1(z_1\cos\Omega\tau - z_2\sin\Omega\tau)\right)(\rho x_2 + z_1\sin\Omega\tau + z_2\cos\Omega\tau)\sin\Omega\tau\right] \\
\dot{z_2} &= \frac{\rho^2}{\Omega}\left[\frac{d}{\lambda}(\rho x_2 + z_1\sin\Omega\tau + z_2\cos\Omega\tau)^2\sin\Omega\tau \right. \\
& -\gamma(z_1\sin\Omega\tau + z_2\cos\Omega\tau)\sin\Omega\tau \\
& \left. -\frac{\Omega}{\tilde{e}}\left(x_1 - \frac{\Omega\lambda}{\tilde{e}}k_1(z_1\cos\Omega\tau - z_2\sin\Omega\tau)\right)(\rho x_2 + z_1\sin\Omega\tau + z_2\cos\Omega\tau)\cos\Omega\tau\right], \\
& && (109)
\end{aligned}$$

The system (108) has the same symmetry as identified in the case I. If we are only interested in solutions with definite parity, we may again start the iteration with $\vec{X_0} = (0, a_2, 0, a_4)$. To the second order ($\rho^2$), the determining equations are:

$$a_2\frac{\lambda e}{a} - \rho\frac{da_4^2k_1}{2\tilde{e}} + O(\rho^3) = 0 \qquad (110)$$

$$\rho\frac{\gamma a_4}{2\Omega} - \rho^2\left(\frac{da_2a_4}{\lambda\Omega} + \frac{\lambda\Omega a_2a_4k_1}{2\tilde{e}^2}\right) + O(\rho^3) = 0. \qquad (111)$$

From the second equation we obtain either $a_4 = 0$ (trivial for our purposes, as discussed above) or

$$\gamma - \rho a_2\left(\frac{2d}{\lambda} + \frac{\lambda\Omega^2k_1}{\tilde{e}^2}\right) + O(\rho^2) = 0. \qquad (112)$$

If we backtrack the transformations made, it is clear that the *consistency condition* requires that we keep terms up to the fourth order (ρ^4). We find that with the substitution

$$e = \frac{\alpha\omega + \mu}{1 + \alpha\beta} + \rho^2(\rho^2\omega_3 - \rho d a_2)\,,$$

where ω_3 is a new parameter, only the fourth or higher order terms are left in the *consistency condition*. From the definition $e = R_0^2 = (\omega - \mu\alpha)/(\beta - \alpha)$ and the above equation, we get $\omega \sim \mu\beta$ and then $e \sim \mu$ to the zeroth order. So $R_0 \sim \sqrt{\mu}$, $q \sim 0$, which means that this solution bifurcates from the HOS $A = \sqrt{\mu}\exp(-i\omega t)$. To the leading order ($\rho^4$), we are allowed to use the following substitutions in the *consistency condition* (98):

$$\begin{aligned} a_2 \to 0 \quad \omega \to \mu\beta \quad \Omega \to \sqrt{-\frac{2\mu(1+\alpha\beta)}{1+\alpha^2}}, \\ k_1 \to \frac{\mu\lambda}{a}\left(1 + \frac{2\lambda(1+\alpha\beta)}{1+\alpha^2}\right) \quad \tilde{e} \to -\frac{2\mu\lambda(1+\alpha\beta)}{1+\alpha^2}\,. \end{aligned} \tag{113}$$

The resulting equation is of a relatively simple form:

$$a_4^2(-\lambda + d^2(1+\alpha\beta)(1+\alpha^2+\lambda+\lambda\alpha\beta)) + 4(1+\alpha\beta)^2\lambda\mu\omega_3 = 0\,. \tag{114}$$

From (110) it follows that a_2 is of order ρ, and from (112) that $\gamma \sim O(\rho^2)$. After a change of variable $a_2 = \rho\, a_{22}$ and keeping only the highest order for the equations, we can rewrite (110) and (112) as

$$a_{22}\frac{\lambda e}{a} - \frac{k_1 d a_4^2}{2\tilde{e}} = 0\,, \tag{115}$$

$$\gamma = 0. \tag{116}$$

For $e, \tilde{e}, k_1$ we use the values in (113). From (115), (116) and (114), we can solve for a_{22}, γ, ω_3. The Jacobian of those equations is

$$J = \begin{pmatrix} \frac{\lambda e}{a} & 0 & 0 \\ 0 & 1 & 0 \\ 0 & 0 & 4(1+\alpha\beta)^2\lambda\mu \end{pmatrix},$$

So, $\det J = 4(1+\alpha\beta)^2\lambda^2\mu e/a \neq 0$ for $1 + \alpha\beta \neq 0$. According to Theorem C.0.2, we have proved that equations (77) and (78) possess periodic solutions.

4.5 Analytic form of periodic solutions, stability analysis and numerical tests

We have proved in the preceding section the existence of symmetric periodic solutions in case I and II. In both cases, a small parameter ϵ or ρ ensures the convergence of successive approximations. However, we did not give a bound on the allowable value of this parameter, nor did we show that the solutions which we obtain are the ones observed in numerical simulations. In this section we give the approximate analytical form of periodic solutions. We compare them with direct numerical integration of the CGLe in case II.

The solutions are shown to be independent of λ to order ϵ in case I and to order ϵ^2 in case II. In addition, these solutions should also satisfy the $3-d$ ODE mentioned in section 4.2 which do not contain λ, so they can be matched with the solutions of the $3-d$ system in a unique way, independent of the value of λ. Hence, we conclude that to all orders the physical solutions are identical for the two values of λ.

The two cases are taken separately. In this section, we reinstate x as the spatial variable, $R = R(x)$.

4.5.1 Case I

Using (82), (99) and the case I calculations of the preceding section, we have after some algebra:

$$\begin{aligned} R^2 &= -2\epsilon d a_2(1 \pm \cos\Omega x) \qquad (117) \\ \phi_x &= -\frac{\epsilon a_2}{2(1+\alpha^2)\Omega}\frac{\sin 2\Omega x \pm 2\sin\Omega x}{1 \pm \cos\Omega x}\,. \end{aligned}$$

To the first order of ϵ, R and ϕ_x are independent of λ. The $\pm$ sign selects two solutions which transform into each other by translating a half period. This is reminiscent of the spatial translation invariance in the symmetric solution space. From the definitions of e, Ω and from (100), (95), we get to the first order:

$$\begin{aligned} \omega &= \mu\alpha - 3\epsilon a_2 \\ \omega_1^2 &= 4\mu + \frac{6\epsilon d a_2}{1+\alpha^2}(\alpha\beta + 2\alpha^2 + 3) \\ \Omega &= \omega_1 + \frac{\epsilon\gamma}{2\omega_1}\,. \qquad (118) \end{aligned}$$

We see that ω and Ω are independent of λ. On the other hand, for periodic boundary conditions, we can use Fourier modes directly to transform the PDE (70) to a finite set of approximate ODE's by Galerkin truncation. Then the stationary solution can be obtained by solving a set of nonlinear algebraic equations.

4.5.1.1 Numerical comparison

If we take as an example the following parameter values (previously used in [163]) for which defect chaos is expected (in the thermodynamic limit):

$$\alpha = 1.5, \quad \beta = -1.2$$

and fix the size of the domain to $L = 24$, then at $\mu = 0.072644$, $\omega = 0.097879$, a periodic solution of period $L/2$ is found. This solution has $R_{max} \simeq 0.0750$. On the other hand, if we use the same α, β, μ and search for $R_{max} \simeq 0.075$ by adjusting ϵ (we always keep $a_2 = 1$), we find that

$$\epsilon \sim 0.00380, \quad \omega = 0.097566, \quad \text{period } \frac{2\pi}{\Omega} = 12.0102\,.$$

The approximate analytic solution and the numerical solution of the exact CGLe agree very well. The profile of R from our successive approximation is shown in Fig. 11.

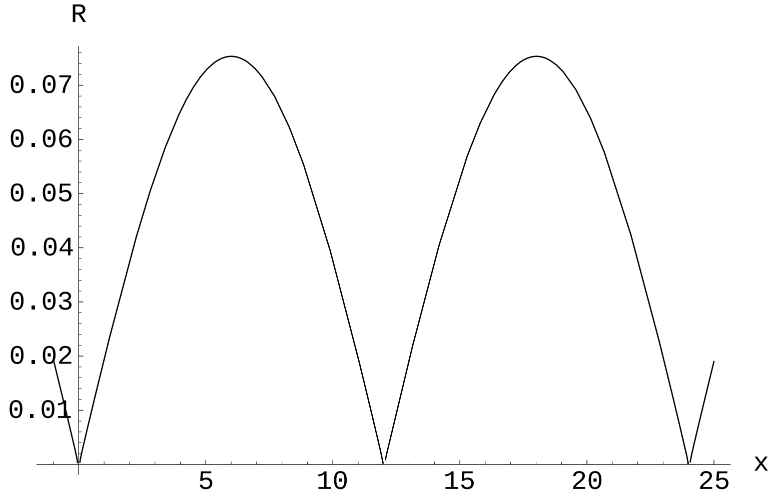

Figure 11: Spatial profile of the amplitude $R(x)$ from (117) at $\mu = 0.07264$, with $R_{\mathsf{max}} = 0.075$.

4.5.1.2 Analytic structure near the defect

It is easy to see from (117) that only $\epsilon a_2 > 0$ is the physically interesting combination. However, we may wonder whether it is really true that $R^2 = dP + e$ remains non-negative everywhere while touching zero at isolated points. Fig. 11 and the first equation of (117) suggest a positive answer to this question. But since we have only an approximate solution, further justification is needed. Suppose at some instant x_0, we have $dP + e = 0$ on the periodic orbit. From the *consistency condition* (98), at this transition point

$$\frac{d^2(1+\alpha^2)}{4}Q^2 + \left(\frac{a}{\lambda}\tilde{N} - \lambda Q\right)^2 = 0,$$

so, $Q = \tilde{N} = 0$. According to (94), $\dot{\tilde{M}} = 0$ and $\dot{P} = 0$. Assume that $\dot{Q} = 0$, then $\dot{\tilde{N}} \neq 0$ since the transition point is not an equilibrium. At next instant $x_0 + \delta x$, the *consistency condition* can not be satisfied as the two sides of (98) have different orders of δx. So we conclude that $\dot{Q} \neq 0$ at the point x_0, which means that $Q(x_0 + \delta x)$ has negative sign to that of $Q(x_0 - \delta x)$. Thus, after touching the zero value hyper-plane, $dP + e$ returns to the positive half space again. The turning happens exactly on the $dP + e = 0$ plane. We claim that $dP + e \geq 0$ always holds and the equality holds periodically for the periodic orbit under consideration. From (117), in the neighborhood of $R = 0$ at $x = x_0$ on the periodic orbit, R behaves like

$$R \sim \left(\frac{d\dot{Q}}{2}\right)^{1/2} |x - x_0|\,,$$

and is manifestly a non-analytic function of x.

We do not discuss the stability of the solutions in case I, as this has already been accomplished by Takáč [248] who has proven that these solutions are unstable.

4.5.2 Case II

To the first order of ϵ, the solutions are

$$\begin{cases} x_1 &= -\frac{\epsilon k_1 a_4^2}{8\tilde{e}^2\Omega}(2d\tilde{e}+\lambda k_3)\sin 2\Omega x \\ x_2 &= \epsilon(a_2^2 - \frac{\lambda k_1 a_4^2}{4\tilde{e}^2}\cos 2\Omega x) \\ z_1 &= -\frac{\epsilon a_4^2}{12\tilde{e}^2\lambda\Omega^2}(3(3d\tilde{e}^2+\lambda^2\Omega^2 k_1)\sin\Omega x + (d\tilde{e}^2 - \lambda^2\Omega^2 k_1)\sin 3\Omega x) \\ z_2 &= a_4 + \frac{\epsilon a_4^2}{12\tilde{e}^2\lambda\Omega^2}(3(\lambda^2\Omega^2 k_1 - d\tilde{e}^2)\cos\Omega x + (\lambda^2\Omega^2 k_1 - d\tilde{e}^2)\cos 3\Omega x)\,, \end{cases}$$

where $\epsilon = \rho^2 > 0$, and a_4 is a free parameter. In the following, we will see that ϵ and a_4 always emerge in the combination $\epsilon\, a_4$ for physical quantities. To the second order, ω is

$$\omega = \mu\beta + \frac{\epsilon^2 a_4^2}{4\mu(1+\alpha^2)}\left(\frac{1+\alpha\beta}{\beta-\alpha} + \frac{\beta-\alpha}{1+\alpha\beta}\right).$$

It is independent of λ, and therefore e, b, Ω are also independent of λ. R and ϕ_x can also be calculated to the second order:

$$\begin{aligned} R^2 &= -\frac{d^2}{2\mu}(\epsilon a_4)^2 + d\epsilon a_4\cos\Omega x + \frac{d(\epsilon a_4)^2}{12\Omega^2}\left(\frac{c}{a}+\frac{e}{b}\right)\cos 2\Omega x + e \\ \phi_x &= \frac{\epsilon a_4}{\mu\Omega(1+\alpha^2)}\left[e\sin\Omega x - \frac{\epsilon a_4}{24\Omega^2}\left(6d\Omega^2 + \frac{7e^2}{a\Omega^2} + \frac{7ce}{a}\right)\sin 2\Omega x\right] \end{aligned} \tag{119}$$

So clearly R and ϕ_x are independent of λ. Similarly, the different signs of a_4 will give the same solution up to a half-period translation. This solution is the one observed in the numerics when passing the Eckhaus instability for underlying wavevector $q = 0$. Linear stability analysis reveals [174] that the $q = 0$ state, the most stable state under the long wavelength perturbations, becomes unstable when the size of the system is such that the smallest possible nonzero wavenumber k satisfies

$$k^2 < -\frac{2\mu(1+\alpha\beta)}{1+\alpha^2} \equiv \kappa^2\,.$$

It is easy to see that $\kappa^2 = \omega_1^2$ up to order (ρ^4).

For our parameter choices $\mu = 1, \alpha = 1.5, \beta = -1.2$, the bifurcation size of the system is $L_0 = \frac{2\pi}{\kappa} = 8.95492$. In the following, we will first prove the stability of our solutions near the bifurcation point. Then we will compare them with the stable solutions observed in numerics.

4.5.2.1 Stability analysis

Assume that $A = R\exp(i\phi)$ where $R, \phi \in \mathbb{R}$ is an exact solution of (70). The perturbed solution is assumed to be $\bar{A} = (R+r)\exp i(\phi+\theta)$, where $r, \theta \in \mathbb{R}$ is the perturbation on the amplitude and phase, separately. Substitute it into (70), keeping only the linear terms in r and θ. We have

$$\begin{aligned} r_t &= (\mu - \phi_x^2 - \alpha\phi_{xx} - 3R^2)r + r_{xx} - 2\alpha\phi_x r_x \\ &\quad -(2R\phi_x + 2\alpha R_x)\theta_x - \alpha R\theta_{xx} \end{aligned} \tag{120}$$

$$\begin{aligned} R\theta_t &= (\omega - \alpha\phi_x^2 + \phi_{xx} - 3\beta R^2)r + \alpha r_{xx} + 2\phi_x r_x \\ &\quad +(2R_x - 2\alpha R\phi_x)\theta_x + R\theta_{xx}\,, \end{aligned} \tag{121}$$

where in (121) we have used $\phi_t = -\omega$. To study the stability of the starting solution A, we treat these equations as an eigenvalue problem for a two-component vector, *i.e.*, we let $r_t = \sigma r$, $\theta_t = \sigma\theta$ and investigate the spectra σ of the linear operator resulting from (120) and (121) in the C^1 continuous periodic function space. As the CGLe has global phase invariance, the eigenvalue equations always have solution $(r, \theta) = (0, \theta_0)$ with eigenvalue $\sigma = 0$. At the same time, spatial translational invariance implies that another eigenmode has $\sigma = 0$. As a result, saying that the solution is stable means that it is stable up to a phase and a spatial translation, and that all other eigenmodes have eigenvalues with negative real parts.

Invoking the expression for R, ϕ_x to the second order of ϵ, the coefficients of various terms of r, θ and their derivatives in (120) and (121) become explicit functions of x. The resulting linear operator on (r, θ) has even parity due to the symmetry of our solution, and we can consider the even and odd modes of r, θ separately. If we set $\epsilon = 0$, i.e., the starting state A is a plane wave state, then $\cos(n\Omega x)$ and $\sin(n\Omega x)$ are the eigenfunctions of the unperturbed linear operator. They give the stability spectrum of the plane waves. Now, let us move a little (to the order of ϵ) beyond the bifurcation point. The eigenfunctions are still $\cos(n\Omega x)$ and $\sin(n\Omega x)$ up to ϵ corrections. For example, if the even solutions are considered first, we assume that to the first order the eigenfunctions are (the time dependence for r, θ has been suppressed):

$$r = m_1\cos(n\Omega x) + \epsilon(m_0\cos((n-1)\Omega x) + m_2\cos((n+1)\Omega x)) \tag{122}$$

$$\theta = n_1\cos(n\Omega x) + \epsilon(n_0\cos((n-1)\Omega x)) + n_2\cos((n+1)\Omega x))\,, \tag{123}$$

where n is a non-negative integer. Note that we do not include the terms such as $\epsilon^2\cos((n\pm 2)\Omega x)$ in the above expressions because they induce corrections of order ϵ^3 or higher in the eigenvalues. Now if we substitute (122) and (123) into the eigenvalue equations and identify the coefficients of $\cos(n\Omega x), \cos((n-1)\Omega x)$ and $\cos((n+1)\Omega x)$, a set of six homogeneous linear equations for $m_0, m_1, m_2, n_0, n_1, n_2$ can be derived. The determinant of the coefficient matrix will give an eigenvalue equation for σ. The resulting expression is too complicated to merit being displayed here.

Before bifurcation, the HOS is stable. The first instability occurs for $n = 1$ mode, one eigenvalue of which is very close to 0 near the bifurcation point, being negative before and positive after. Meanwhile, for $n > 1$ modes, the corresponding eigenvalues have negative real parts bounded away from zero. As the bifurcating solution emerges continuously from the HOS, near the bifurcation point ($\epsilon \ll 1$) the perturbed linear operator has all the eigenvalues with negative real parts away from 0 for $n > 1$ and one eigenvalue close to 0 for $n = 1$. So, we only need to check the stability of our solutions for $n = 1$.

For convenience, we can fix parameters α and β to any values allowed by (97) and perform the above stability analysis of the solution.

The numerical values we used are $\mu = 1.0, \alpha = 1.5, \beta = -1.2, a_4 = 1$. The eigenvalue equation is then

$$\begin{aligned} 7.9860\epsilon^2\sigma + (56.423 - 63.394\epsilon^2)\sigma^2 + (82.564 - 75.135\epsilon^2)\sigma^3 \\ +(45.022 - 28.859\epsilon^2)\sigma^4 + (10.923 - 4.3059\epsilon^2)\sigma^5 \\ +(1.0 - 0.18864\epsilon^2)\sigma^6 &= 0\,. \end{aligned}$$

$\sigma = 0$ corresponds to the neutral mode associated with the global phase invariance. All others solutions have negative real parts. The $\sigma_- = -0.14154\epsilon^2$ solution is the interesting one. If we use the same parameter values to calculate the stability of the HOS, the eigenvalue equation for $n = 1$ is

$$\epsilon^2(-0.21122 - 0.26402\sigma) + 2.98462\sigma + \sigma^2 = 0\,.$$

To the second order in ϵ, we have $\sigma = -2.98462 - 0.19325\epsilon^2$ or $\sigma_+ = 0.07077\epsilon^2$. The later positive eigenvalue indicates that the plane wave solution is not stable. We note that $2\sigma_+ = -\sigma_-$ to order ϵ^2 which indicates a supercritical pitchfork bifurcation. We have proved that this equality holds exactly at the bifurcation point for any values of α and β, and this justifies the above numerical checks. Under perturbation the HOS will evolve to the modulated amplitude solution given above. When the instability is saturated, the corresponding eigenvalue for the MAW is negative. If we change the sign of a_4 or use the other value of λ, the eigenvalue does not change, as expected.

If we alternatively consider the odd-parity function space $\{\sin(n\Omega x)\}_{n\in\mathbb{N}}$, we obtain the following eigenvalue equation:

$$\begin{aligned} (28.2115 - 33.6568\epsilon^2)\sigma + (27.1763 - 21.2703\epsilon^2)\sigma^2 + (8.92308 - \\ 4.04125\epsilon^2)\sigma^3 + (1 - 0.19287\epsilon^2)\sigma^4 = 0\,. \end{aligned}$$

This equation is quartic because for $n = 1$ only two modes $\sin\Omega x$ and $\sin 2\Omega x$ are used. Now $\sigma = 0$ corresponds to the neutral mode associated with the spatial translation of the CGLe. Other eigenvalues of the equation have negative real parts bounded away from 0.

To summarize, our solution is stable in the whole phase space of the CGLe, up to a phase and a spatial translation.

In ref [136], B. Janiaud *et al.* have investigated the stability of traveling waves near the Eckhaus instability in Benjamin-Feir stable regime. They derived a necessary condition for the bifurcation to be supercritical and located the corresponding regions as two strips in the α, β parameter space. We have studied the stationary MAWs in the Benjamin-Feir unstable regime and found that the bifurcation from the HOS to MAWs is always supercritical, even when parameter values lay outside of the region given in ref [136].

In ref [193], application of the perturbation method to the zeroth order (ϵ^0) equation gave nonzero eigenvalue $\lambda_0 = 2/\beta$. This can not be correct since the zeroth order equation just gives the stability of the unstable HOS. Furthermore, in the Galerkin projection calculation in [193], somewhat surprisingly the $N = 1$ truncation was found to give a better result than the $N = 2$ truncation. In our case, if we used only the first order expressions for R, ϕ_x in (120) and (121), we could not get the correct eigenvalues even near the bifurcation point, and thus are absolutely forbidden to extend the result to the next bifurcation.

4.5.2.2 Comparaison with numerical integration of the CGLe

In our numerical simulations we employed a pseudo-spectral method to evolve equation (70) using 128 modes. For system size $L < L_0$, we always recover the HOS ($q = 0$). For L slightly larger than L_0, however, the solution relaxes to the modulated amplitude solution (119) for any smooth initial condition we have tried. Figure 12 compares the stable steady solutions obtained by the two methods.

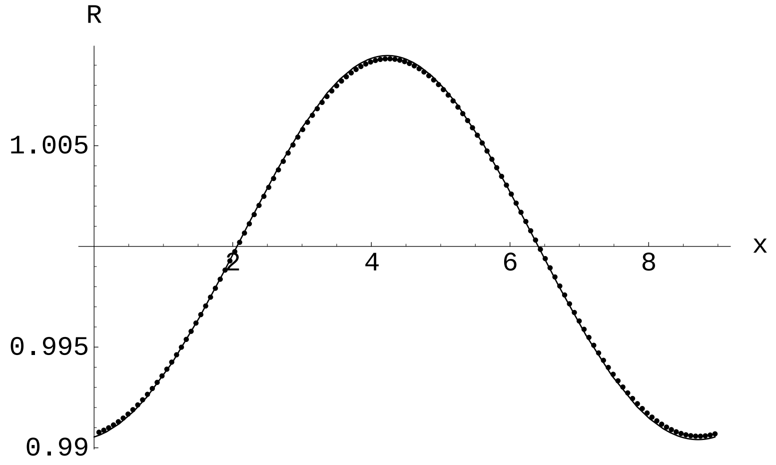

Figure 12: Spatial profiles of the amplitude R for $\mu = 1, \alpha = 1.5, \beta = -1.2, L = 8.958$ from numerical simulation (dots) and the approximate solution (119) (solid line). The agreement is good, with the discrepancy mainly due to the long relaxation time close to the bifurcation point.

4.6 Summary

After reviewing the basic properties of the 1-d CGle, we reformulated the equation for its stationary solutions as a fourth-order ODE for a variable P that can be interpreted as the modulation of the amplitude squared of a plane wave solution. This reformulation enabled us to prove the existence of stationary MAW solutions in the two limit cases corresponding to the bifurcation of the trivial solution $A = 0$ (case I), and to the bifurcation of the plane wave solution of zero wavenumber (case II).

We proved the stability of MAW solutions for the full CGLe in a finite box with periodic boundary conditions in case II near the onset of plane wave instability. We tested our analytical results by comparison of numerical integrations of the full CGLe with our approximate analytical solutions.The MAWs continue to exist when the size L is increased. In case I, unstable periodic hole solutions were shown to exist. This could not be inferred from any phase equation: around the defect point $A = 0$, the amplitude behaves non-analytically, namely piecewise affinely, and the phase is not defined.

The analysis of MAWs bifurcating from a plane wave with wavenumber $0 < q < 1$ should be similar to the study of case II. It would be interesting to study the higher order instabilities of MAWs when the system size is increased beyond the region in which our analysis takes place. It has been observed that stationary symmetrical MAWs bifurcate into uniformly-propagating asymmetrical ones via a drift-pitchfork bifurcation. This happens when L is increased as a consequence of the growth of the amplitude of the modulation, and the increase of the spectral richness of the MAW solution. Moreover, MAWs are expected to be the building blocks of phase turbulence, and the analytical analysis of their global stability may lead to a characterization of the suspected transition between phase and defect chaos in the CGLe [30, 28].

Complex Ginzburg-Landau equation—)